doi:10.2489/jswc.2022.00037

Effects of rainfall intensity and slope gradients on total carbon, nitrogen, and phosphorus lateral transport under simulated extraordinary rainstorm

K. Fei, T. Sun, L. Deng, L. Zhang, Y. Wu, X. Fan, and Y. Dong

Abstract: The aim of this research was to study the characteristics and influence of the lateral transport of total carbon (TC), total nitrogen (TN), and total phosphorus (TP) under different slope gradients (5°, 8°, 15°, 25°) caused by extraordinary rainstorms (90 mm h^{-1}, 120 mm h^{-1}, 150 mm h^{-1}) on a decomposed granite soil in the Zhejiang-Fujian hilly region. Rainfall induced runoff (RIR) contains overland flow (OF) and interflow (IF). Results show that with the increase of runoff time and runoff volume, TN and TP mass concentrations decrease rapidly; however, TC mass concentration increases with the increase of runoff volume in IF. TC mass concentrations greater than 55 mg L^{-1} are distributed in areas with IF volume more than 5,100 mL. Meanwhile, a marginal effect of TC, TN, and TP increments appeared when examining TC, TN, and TP cumulative loss amounts in RIR; the inflection points appeared at the end of rainfall event. A simple stoichiometry was applied. Simulated rainfall reduced the C:N ratio with a range from 6.68 to 5.98 while increasing the C:P and N:P ratios when rainfall intensity was 120 or 150 mm h^{-1}. Sediment is the main carrier for C lateral transport. We also noted that the gross amount of TC loss in RIR accounted for more than 10%. The loss of TC with runoff cannot be ignored. Our research enriches slope land hydrology research under extraordinary rainstorm conditions and provides a basis for the effective control of TC, TN, and TP loss in the decomposed granite soil area of China and globally.

Key words: C:N:P stoichiometry—decomposed granite soil—interflow—simulated extraordinary rainstorm—slope gradient—soil nutrients

Decomposed granite soils are widely distributed in the hilly area of southeast China and are subjected to the compound action of runoff and gravity erosion with huge nutrient loss. This greatly limits the sustainable development of the ecological environment and the social economy (Fujimoto et al. 2007; Katsuyama et al. 2010). Furthermore, there are often short-term extraordinary rainstorm events caused by typhoons in southeast China (Xu et al. 2019). Research studies on decomposed granite soil slopes have mostly focused on the runoff process and sediment transport under medium and low rainfall intensity. However, there are few studies on the process and characteristics of nutrient loss under extraordinary rainstorm events (Chang et al. 2021; Zheng et al. 2017).

Rainfall intensity and slope gradient are known to be the two most important external factors that affect rainfall-induced runoff and sediments, and ultimately soil nutrient loss (Chaplot and Le Bissonnais 2003; Huang et al. 2013). Research results on the effect of rainfall intensity on nutrient loss or lateral transport are relatively consistent. The increase of rainfall intensity will increase runoff volume, the amounts of sediments, and total carbon (TC), total nitrogen (TN), and total phosphorus (TP) losses (Kleinman et al. 2006; Ramos et al. 2019; Wu et al. 2021). The impact of slope gradient is more controversial. Most researchers believe that the greater the slope gradient, the greater the amount of nutrient loss. When slope gradient increases, the flow velocity will increase, and the runoff volume and amount of sediment will increase, thereby increasing the amount of nutrient loss (Rimal and Lal 2009; Wu et al. 2018). Some studies have pointed out that different nutrients in the soil present different loss characteristics with rainfall-induced runoff and sediment (Korkanç and Dorum 2019; Ramos et al. 2019). For instance, TN, with more negative charge, is easy to transport with runoff, while TP, with positive charge, is easy to lose with sediment and TC is mostly transported with sediment because it is insoluble in water. However, the loss characteristics of these nutrients under extreme rainstorm conditions are not clear in a decomposed granite soil area.

Loss of C, N, and P on slopes not only pollutes waterways, but may inhibit the growth of plants (Huang et al. 2017; Shen et al. 2013). During the internal cycle of the ecosystem, they are independent and interconnected. Plant C sequestration occurs primarily through photosynthesis, which is affected by the content of N and P, and N and P are the main limiting elements that affect plant growth (Ross et al. 1999; Wang and Moore 2014). To account for this, we introduce the concept of stoichiometry. Different stoichiometric ratios have different responses to different environmental factors (Ågren and Weih 2012; Cleveland et al. 2007). It plays an important role in revealing the availability of nutrients and the circulation and balance mechanisms of C, N, and P (Schipper et al. 2004). It is also the main indicator reflecting the soil C, N, and P cycles. Stoichiometry

Received March 3, 2021; Revised December 15, 2021; Accepted January 17, 2022.

Kai Fei is a PhD student, **Tianyu Sun** is a PhD candidate, and **Longzhou Deng** is a PhD candidate at the Institute of Soil and Water and Environmental Sciences, College of Environment and Resource Sciences, Zhejiang University, Hangzhou, China. **Liping Zhang** (corresponding author) is a professor at the Zhejiang Provincial Key Laboratory of Agricultural Resources and Environment, Hangzhou, China. **Yanhong Wu** and **Xiaojuan Fan** are master's students at the Institute of Soil and Water and Environmental Sciences, College of Environment and Resource Sciences, Zhejiang University, Hangzhou, China. **Yayue Dong** is a master's student at the College of Foreign Language and Literature, China Youth University of Political Studies, Beijing, China.

can measure and integrate the variability of ecosystem functions and can also help determine the response of ecological processes to global changes.

Above all, this study uses the artificial rainfall simulation method to examine the combined effects of slope gradient and rainfall intensity. By measuring the characteristics of the flow process and TC, TN, and TP mass concentration in overland flow (OF) and interflow (IF) during rainfall, the dynamic curves of TC, TN, and TP loss rate were obtained. Using stoichiometry, we analyze the effects of TC, TN, and TP loss on slope soil C, N, and P, and explore mechanisms of the gross soil TC, TN, and TP losses due to rainfall intensity, slope gradient, rainfall induced runoff (RIR), and sediments. Our goal is to reveal the loss characteristics and influencing factors of TC, TN, and TP and provide a theoretical basis for the reasonable allocation of soil erosion control measures on decomposed granite soil areas in the Zhejiang-Fujian hilly region.

Materials and Methods

Soil Samples. The decomposed granite soils used in this study were collected from the city of Huzhou, Zhejiang, China (figure 1). Decomposed granite soils belong to laterite, and granites are the main parent materials of laterite. Decomposed granite soils are widely distributed in the Zhejiang-Fujian hilly region. According to the statistics of landslides in southeast coastal areas from 1990 to 2009, most geological disasters occurred in the granite weathering crust area of southeast China (Jiang et al. 2010).

Previous studies have shown that decomposed granite soil can be divided into surface layer, exposed laterite layer, exposed sand layer, and exposed debris layer (Deng et al. 2020a; Wang et al. 2016; Duan et al. 2021) (figure 2). The laterite layer would be exposed when the surface layer is eroded, and the sand layer would be exposed when the laterite layer is eroded. Therefore, the soil used in this study is collected from the surface. According to the Food and Agriculture Organization of the United Nations soil texture classification, sand layer soil belongs to sandy loam soil (Deng et al. 2020a; Jahn et al. 2006). Soils sampled from the exposed sand layer were used. The method for relocating the undisturbed soil was to collect soil every 5 cm to a depth of 60 cm using a spade in the five selected representative sampling plots.

Figure 1
Sampling area.

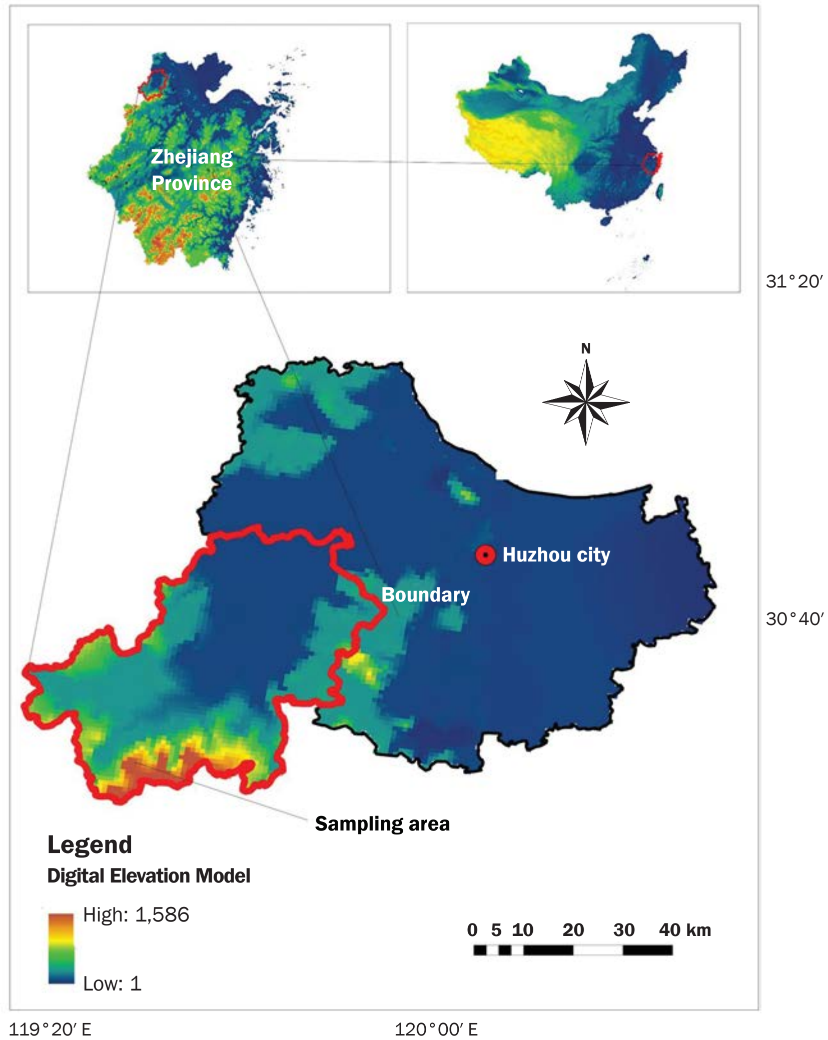

The collected soils were carefully loaded to ensure that the soil structure was not damaged as much as possible. Then the soils in the sampling plots were collected by cutting rings (250 cm^3) and dried to a constant mass at 105°C to determine bulk density based on the volume-mass relationship.

A total of 12 artificial rainfall tests were conducted in six months. Before the first test began, the soil was filled and compacted according to the corresponding undisturbed soil bulk density of the corresponding layer × volume (5 cm × 100 cm × 200 cm) in the test flume. Care was taken to ensure that the soil bulk density in the test flume was the same as the undisturbed soil. Then the flume was left to rest and settle in the laboratory for around 7 days and outside for around 38 days to gradually return soils to the natural state.

The original soil was collected for the measurement of basic physical and chemical properties (table 1). The interval of each test was one week. After testing, the test flume was raised to a certain angle to discharge the flowing water in the soil to ensure that the water moisture (9% ± 1%) of the soil was consistent before each test.

Rainfall Simulation Experiments. The study was conducted at Zhejiang University Agricultural Non-Point Source Pollution and Soil Erosion Control Artificial Rainfall Simulation Base in the Zhejiang University Agricultural Science Experiment Station (Changxing, China). Innovative variable slope three-dimensional monitoring test flumes were used for the simulation (Zhang et al. 2017) (figure 3a). A total of two test flumes were used, and the two test flumes were arranged in parallel (figure 3b). The test flume specifications for length, width, and height are 2 m, 1 m, and 0.6 m, respectively. Hydraulic devices were used to control the slope gradient of the flume. The top of the flume was provided with a triangle outlet, which collected the OF samples and sediments. Moreover, a total of 3 faucets were placed every 20 cm from the top to the bottom with 12 outlets set equally on each side to discharge IF. Soil samples were collected in the two test flumes before each rainfall simulation, and the soil moisture content was measured to ensure that the water content of all the simulated soils was relatively consistent.

The rainfall simulator used was the QYJY-501 (502) portable full-automatic stainless steel simulation rainfall device (figure 3). The simulator's height is 6 m. Eight rain shower heads (3 nozzles per group) were set around the flumes to ensure the uniformity of the rainfall. Twenty-four nozzles were used to completely cover the two test flumes to guarantee rainfall uniformity and reduce error. Eight measuring tubes (diameter: 85 mm, height: 200 mm) were also placed around the test flumes for each rainfall simulation to measure the rainfall uniformity. The rainfall intensity was controlled by a fully automatic rainfall controller, resulting in rainfall accuracy of more than 90%. Rainfall intensities in the Zhejiang-Fujian hilly region were widely variable (Ma et al. 2015). The rainfall intensity of most studies is below 90 mm h^{-1}. However, climate change will lead to abnormal precipitation, so it is urgent to study the soil erosion under extremely heavy rainfall. The range of the slope gradients was large, varying from 0° to 24.2° (Shuttle Radar Topography Mission [SRTM] 90 m). According to the rule of equal difference, equidistance between the rainfall levels and Chinese classification standard for potential hazard of soil erosion (SL718—2015), a total of three rainfall intensities and four slope degrees were designed: 90 mm h^{-1} (I90), 120 mm h^{-1} (I120), and 150 mm h^{-1} (I150), with slope gradients of 5° (G5), 8° (G8), 15° (G15), and 25° (G25), respectively.

Overland flow is formed when the soil is saturated by water to its full capacity, or the rain arrives more quickly than the soil can absorb it. Interflow is the shallow, ephemeral subsurface flow through the soil/regolith. The experiment set a simulated test duration of 90 min. At the start of generating OF, water samples were collected in graduated polyethylene bottles every 3 min. After the rainfall simulation was over, the OF was almost finished, so the OF sample was not collected. The tested IF time was about 3 h, so it was set for collection of 120 IF samples at the two flumes.

Fertilization Scheme. According to the common fertilization ratio of local farming, 100 g of organic fertilizer (total organic C accounted for 63.0%, TN accounted for 2.5%, and TP accounted for 3.5%) and 20 g of compound fertilizer (TN accounted for 33.3% and TP accounted for 33.3%) were uniformly broadcasted on the soil surface 7 days before each test. Then some water was sprinkled on the soil surface to blend the fer-

Figure 2
Schematic diagram of soil layers of decomposed granite soil.

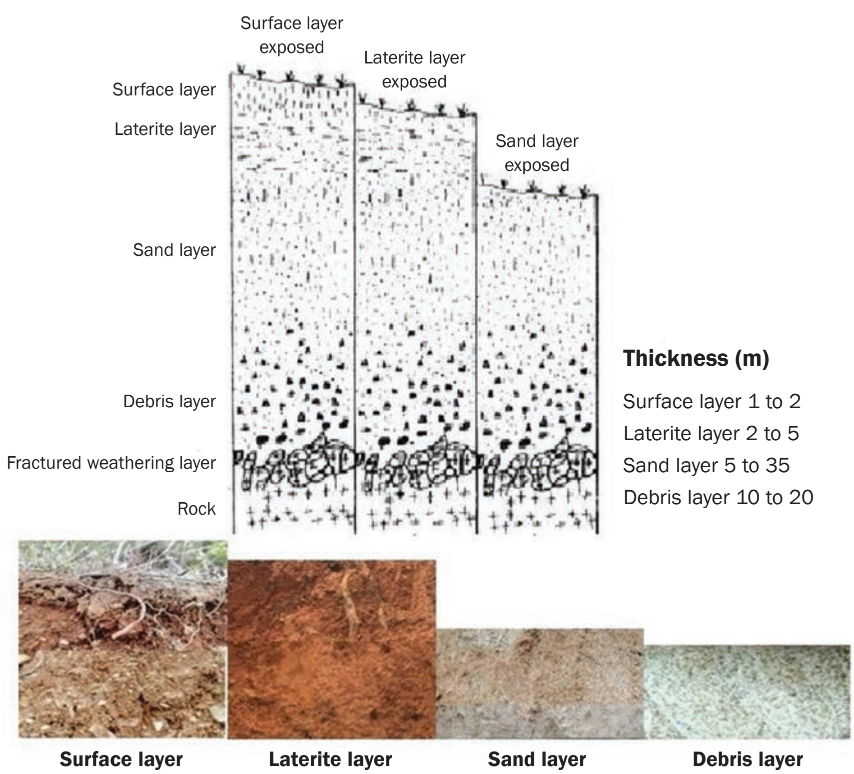

Table 1
Basic physical-chemical characteristics.

Soil depth (cm)	Bulk density (g cm^{-2})	pH	Clay (%; <0.002)	Silt (%; 0.002 to 0.02)	Sand (%; >0.02)	SOC (g kg^{-1})	A-P (mg kg^{-1})	A-K (mg kg^{-1})	TN (g kg^{-1})
0 to 60	1.55	6.22	8.24	12.25	79.52	2.71	10.93	54.53	0.90

Notes: SOC = soil organic carbon. A-P = available phosphorus. A-K = available potassium. TN = total nitrogen. The test data were analyzed and plotted with R-studio 3.6.3, SPSS 20.0 and Origin 2017b.

tilizer with the soil better. The ratio of nitrate (NO_3^-) and ammonium (NH_4^+) of TN in the above fertilizer was as 3.1:1. Balance calculations, commonly used in studies of simulated rainfall (Chen et al. 2008; Tiwari et al. 2010; Brookshire et al. 2009), were employed here using the following formula because the broadcast fertilizer we broadcast could not be completely transported out of the flume in each rainfall experiment (equations 1 to 3 are the balance calculation formulas of TC, equations 4 to 6 are the balance calculation formulas of TN, and equations 7 to 9 are the balance calculations of TP):

$$F_{nTC} = \sum_{i=1}^{n=20} B_{fTC} - \sum_{i=0}^{n=19}(D_{wTC} + S_{dTC}) + S_{TCoriginal} - M_{CO_2}, \quad (1)$$

$$C_{TC}(\%) = \frac{B_{fTC}}{F_{nTC}} \times 100\%, \text{ and} \quad (2)$$

$$TC_{mc}(mg\ L^{-1}) = C_{TC}(\%) \times TC_{mcm}, \quad (3)$$

where F_{nTC} is the total amount of TC before the *n*th simulated experiment, B_{fTC} is the total amount of TC in each fertilizer application, D_{wTC} is TC loss gross amount with RIR, S_{dTC} is TC loss gross amount with sediments, $S_{TCoriginal}$ is the original content of TC, M_{CO2} is the total amount of CO_2 transformation before each rainfall experiment, $C_{TC}(\%)$ is reduction factor, TC_{mc} is the correctional TC mass concentration, and TC_{mcm} is the testing TC mass concentration.

$$F_{nTN} = \sum_{i=1}^{n=20} B_{fTN} - \sum_{i=0}^{n=19}(D_{wTN} + S_{dTN}) + S_{TNoriginal}, \quad (4)$$

$$C_{TN}(\%) = \frac{B_{fTN}}{F_{nTN}} \times 100\%, \text{ and} \quad (5)$$

$$TN_{mc}(mg\ L^{-1}) = C_{TN}(\%) \times TN_{mcm}, \quad (6)$$

where F_{nTN} is the total amount of TN before the *n*th simulated experiment, B_{fTN} is the total amount of TN in each fertilizer application, D_{wTN} is TN loss gross amount with RIR, S_{dTN} is TN loss gross amount with sediments, $S_{TNoriginal}$ is the original content of TN, $C_{TN}(\%)$ is reduction factor, TN_{mc} is the correctional TN mass concentration, and TN_{mcm} is the testing TN mass concentration.

$$F_{nTP} = \sum_{i=1}^{n=20} B_{fTP} - \sum_{i=0}^{n=19}(D_{wTP} + S_{dTP}) + S_{TPoriginal}, \quad (7)$$

$$C_{TP}(\%) = \frac{B_{fTP}}{F_{nTP}} \times 100\%, \text{ and} \quad (8)$$

$$TP_{mc}(mg\ L^{-1}) = C_{TP}(\%) \times TP_{mcm}, \quad (9)$$

where F_{nTP} is the total amount of TP before the *n*th simulated experiment, B_{fTP} is the total amount of TP in each fertilizer application, D_{wTP} is TP loss gross amount with RIR, S_{dTP} is TP loss gross amount with sediments, $S_{TPoriginal}$ is the original content of TP, $C_{TP}(\%)$ is reduction factor, TP_{mc} is the correctional TP mass concentration, and TP_{mcm} is the testing TP mass concentration.

Figure 3
(a) The rainfall simulator and (b) test flume used in this study.

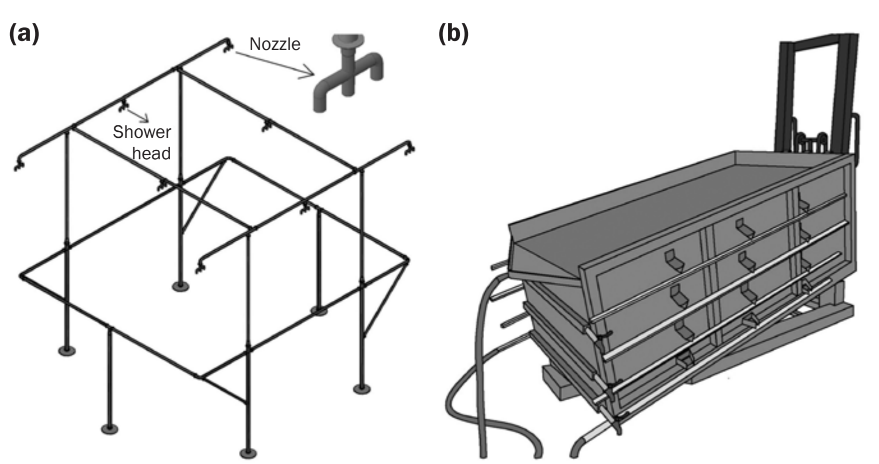

Data Analysis. The following physical and chemical properties of test soils were measured: soil bulk density, pH, soil organic C, total P, and available P (table 1). The methods are strictly based on Chinese soil agrochemical analysis (Bao 2000). Additionally, particle size was measured by hydrometer method (Bouyoucos 1962). At the end of each test, all the OF and IF samples were measured for volume. Due to the large volume of these samples, 250 mL of each sample was collected for chemical analysis within one day. The liquid was taken for TC and mass concentration determination using a TOC analyzer (TOC-4200, Shimadzu Corp., Hong Kong, China). TP mass concentration was measured by determination of total P-ammonium molybdate spectrophotometric method. Then the accumulated TC, TN, and TP loss amounts were determined by calculation as follows:

$$TC_{ca}(mg) = \sum_{i=1}^{n} TC_{mc} \times RV, \quad (10)$$

$$TN_{ca}(mg) = \sum_{i=1}^{n} TN_{mc} \times RV, \text{ and} \quad (11)$$

$$TP_{ca}(mg) = \sum_{i=1}^{n} TP_{mc} \times RV. \quad (12)$$

$TC_{ca}(mg)$ is the accumulated TC loss, $TN_{ca}(mg)$ is the accumulated TN loss, $TP_{ca}(mg)$ is the accumulated TP loss, and RV is the RIR volume per 3 min.

Soil organic C and total P were measured by potassium dichromate volumetric method-external heating method and digestion-Mo-Sb Anti spectrophotometric method, respectively (Bao 2000). Soil total N was measured by determination of total N-Modified Kjeldahl method (Bremner 1960).

Results and Discussion

Variation Characteristics of Total Carbon, Total Nitrogen, and Total Phosphorus Mass Concentration in Overland Flow. We studied the relevance of TC, TN, and TP mass concentrations with OF volume and OF duration (figure 4). OF duration occurred from OF generation to termination of rainfall. TN mass concentration was greater when the OF duration was short with small OF volume. Then TN mass concentration decreased rapidly as the test duration increases. The change process of TP mass concentration is similar to that of TN, but it could be found that higher TP mass concentrations are distributed in the moderate OF volume region. TC mass concentration was larger at the beginning of the rainfall and was still large with small OF volume in the middle and late periods, but it was found that it gradually decreased as the OF volume increased.

Variation Characteristics of Total Carbon, Total Nitrogen, and Total Phosphorus Mass Concentration in Interflow. We also studied the relevance of TC, TN, and TP mass concentrations with IF volume and IF duration (figure 5). IF duration is 180 min. At the initial period of IF duration, TC, TN, and TP mass concentrations were generally higher than that in the middle and late period. Higher TN and TP mass concentrations were distributed in regions of smaller IF volume, and the value of TP mass concentration tended to 0 when the IF volume was larger, while TC mass concentration shows opposite trend, with larger values when IF volume was larger. TC mass concentrations greater than 55 mg L^{-1} were all distributed in the regions with IF volume greater than 5,100 mL. As IF duration increased, TC, TN, and TP mass concentrations decreased gradually; the same trend also appears in IF volume variation.

Characteristic Analysis of Total Carbon, Total Nitrogen, and Total Phosphorus Cumulative Loss Amounts. The characteristics of TC, TN, and TP cumulative loss amounts are shown in figure 6. TC, TN, and TP cumulative loss amounts in RIR showed a rapid increase at the beginning and a slow increase in later period. An inflection point appears at the end of the rainfall. The appearance of the inflection point is called its occurrence of a marginal effect. We regard the simulated duration as an input. After the inflection point, continuously increasing the simulated duration would reduce the new nutrient loss. That is to say, when the input of simulated duration reaches a certain level, the new loss of nutrients from the input of new simulated duration will decrease.

Stoichiometric Characteristics of Soil Carbon, Nitrogen, and Phosphorus after Rainfall. The C:N:P of the remaining nutrients in the soil after rainfall was calculated after balance calculations (table 2). Rainfall caused the C:N ratio to decrease, ranging from 6.68 to 5.98. C:P ratio increased at I120 from 6.05 to 9.90 and I150, with a range of 8.06 to 23.00. The change of N:P ratio was similar with that of C:P, and the change ranges at I120 and I150 were 1.08 to 0.65 and 0.80 to 0.26, respectively.

Figure 4

Variations of (a) total carbon, (b) total nitrogen, and (c) total phosphorus mass concentration with overland flow (OF) volume and test duration in OF. The unit of mass concentration is mg L^{-1}. Larger pattern with lighter color indicates larger value.

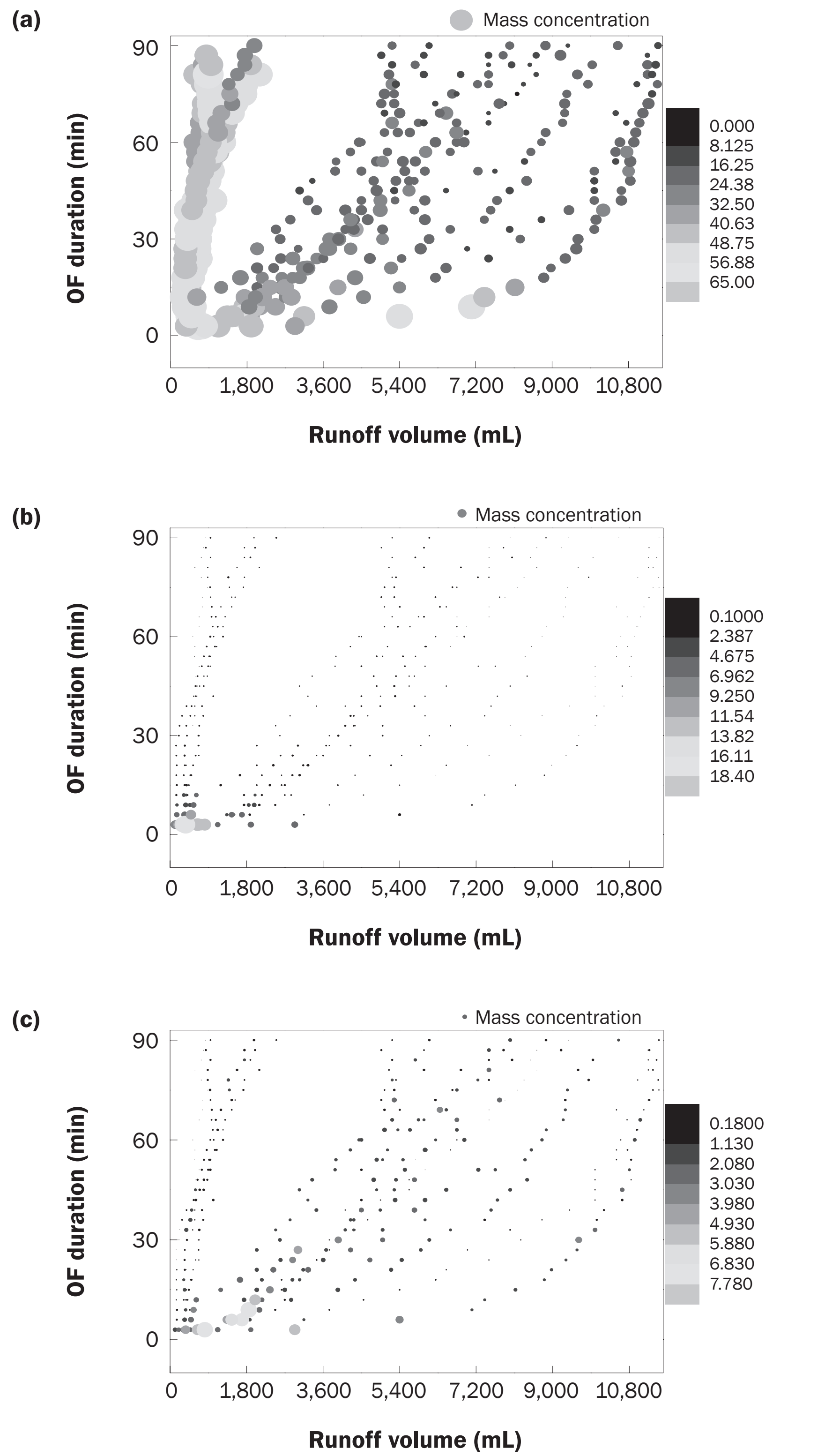

Figure 5
Variations of (a) total carbon, (b) total nitrogen, and (c) total phosphorus mass concentration with interflow (IF) rate and IF duration in IF. The unit of mass concentration is mg L^{-1}. Larger pattern with lighter color indicates larger value.

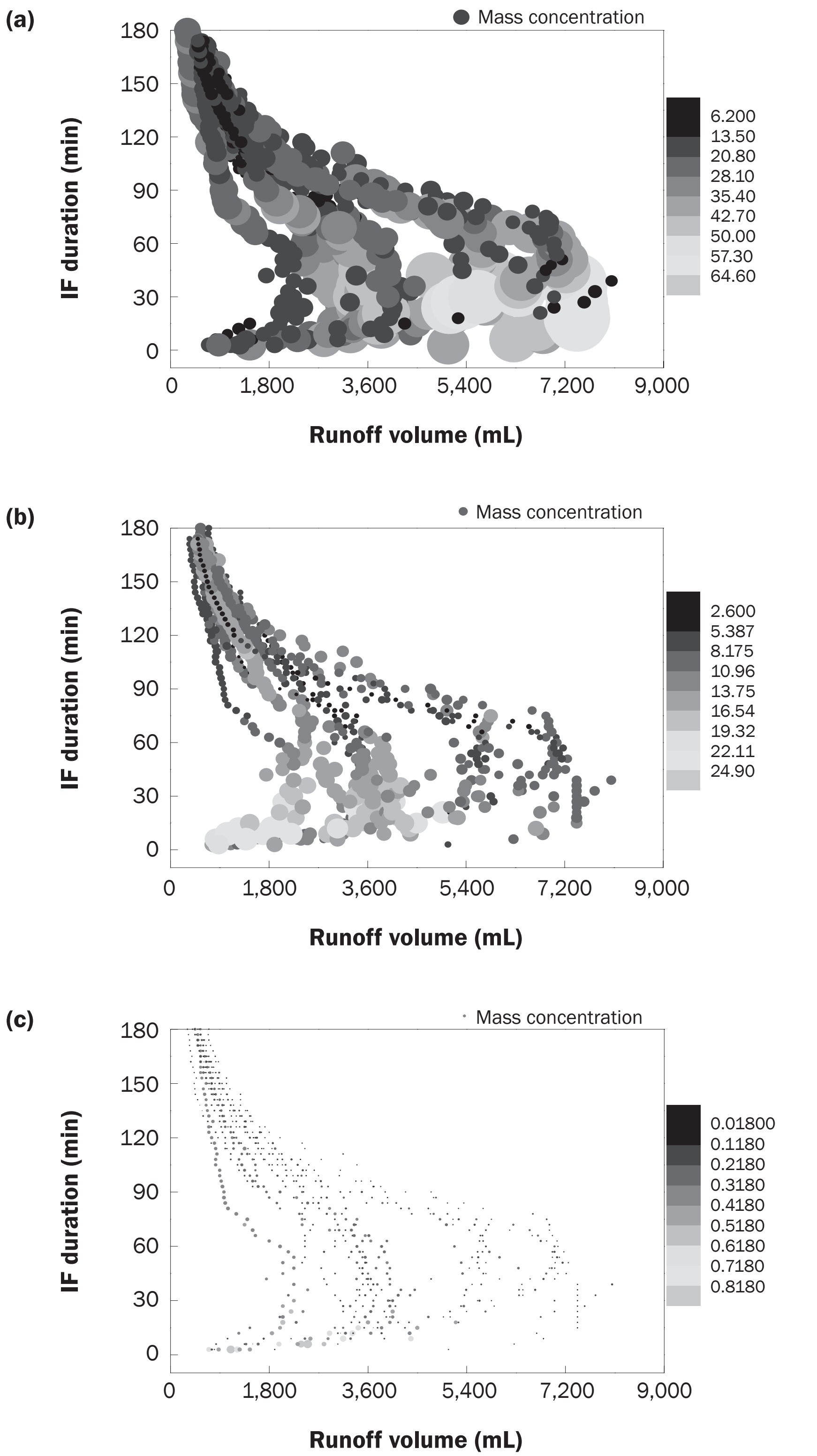

Characteristic Analysis of Total Carbon, Total Nitrogen, and Total Phosphorus Loss Gross Amounts. The comparison of TC, TN, and TP loss gross amounts with OF, IF, RIR, and sediments were studied (figure 7). In RIR, TP was mainly lost with OF except for I90-G5, which accounted for more than 50%. TN was mainly lost with IF, which accounted for more than 90%. TC was lost more with OF when the slope gradient was smaller while it was lost more with IF with the larger slope gradient. Sediments were the main carrier of TC and TP; TP loss gross amount by the sediments accounted for more than 95% of total loss, and TC loss gross amount with sediments exceeded 60%. The loss gross amount of TC in RIR all exceeds 10%. RIR was the main carrier of TN, and the gross amount of TN the RIR carrying accounted for more than 90% of the total loss. At the same time, linear regression showed that under extreme rainfall conditions, TC, TN, and TP loss gross amounts all had significant linear dependence with rainfall intensity. The R^2 of the fit between the predicted value and the measured value was above 0.85 (figure 8).

The Distribution of Total Carbon, Total Nitrogen, and Total Phosphorus Mass Concentration. The first flush effect refers to the high mass concentration of pollutants in the whole OF process during the initial period (Lee and Bang 2000). Similarly, we found that TC, TN, and TP mass concentrations were relatively highest at the beginning of each test. At the middle and late rainfall period, TC, TN, and TP mass concentrations showed a downward trend with the gradual formation of surface crust. Many studies have reached similar conclusions (Qian et al. 2014; Wang et al. 2014; Lang et al. 2013). We have not found a reasonable explanation as to why TC mass concentration was larger when the OF volume was smaller in the middle and late rainfall period. It may be because the fertilization was broadcasted to the surface and the amount of fertilization was relatively high. A large amount of TC was lost along with OF in each period. Therefore, TC mass concentration was still large due to the small dilution effect of smaller OF volume.

The smaller the saturated hydraulic conductivity of the soil, the slower the water infiltration rate, and the more easily the excess water is retained between the soil layers, further forming IF (Goel 2011). IF is composed of macropore flow and matrix flow. Macropore flow is a manifestation of preferential flow, and it forms faster than matrix flow (Petry et al. 2002). At the beginning, the IF is mainly formed by preferential flow, when volume is small. As the matrix flow is gradually supplemented, the volume of OF gradually reaches the maximum, and then it gradually decreases after the rainfall ceases. The large mass concentration of TN and TP in OF were mainly distributed in the region at the beginning of the OF duration with smaller volume. This is due to the slow flow velocity and full interaction between TN, TP, and soil in the early period, so the mass concentration is greater. Of course, because of the reverse charge to P, soil has a strong adsorption of P; the mass concentration of TP in IF was an order of magnitude smaller (Ruby et al. 2016). The large TC mass concentration was mainly distributed at the beginning of the IF duration with large IF volume. Soluble C content is low, so the TC concentration in the early period is low (Boddy et al. 2007). As the IF volume increased, the IF velocity increased continuously, reaching the initial velocity of some suspended C and some colloidal C, so when volume becomes larger, the TC mass concentration increased. After rainfall stopped, the flow velocity slowed down, and the C infiltrating into the soil was consumed, so TC mass concentration slowly decreased until it was stable. Many researchers believe that colloids in RIR will also contain certain nutrients (Gomez-Gonzalez et al. 2016). The velocity was not studied in this experiment, but former studies have shown that there was a strong positive significant correlation between flow velocity and the RIR volume, and the nutrient loss increases with the increase of RIR volume (Liu et al. 2018; Xu et al. 2018; Liu et al. 2017).

Impact of Rainfall on Carbon:Nitrogen:Phosphorus Ratio. Due to the differences in soil adsorption of various nutrients, the effect of heavy rainfall on the washing of nutrients will be different, so the C:N:P ratios in the soil will also change after rainfall. The ratio of C:N:P in the soil will remain relatively stable, which is closely related to the soil microorganisms, vegetation, and climate. However, this study shows that nutrient loss caused by extreme rainfall can rapidly change its proportion, which will accelerate the process of soil degradation, and it will take a long time for ecological restoration to return to the natural level (Du and Gao 2021).

Figure 6

(a) Total carbon (TC), (b) total nitrogen (TN), and (c) total phosphorus (TP) cumulative loss amounts in rainfall induced runoff (RIR).

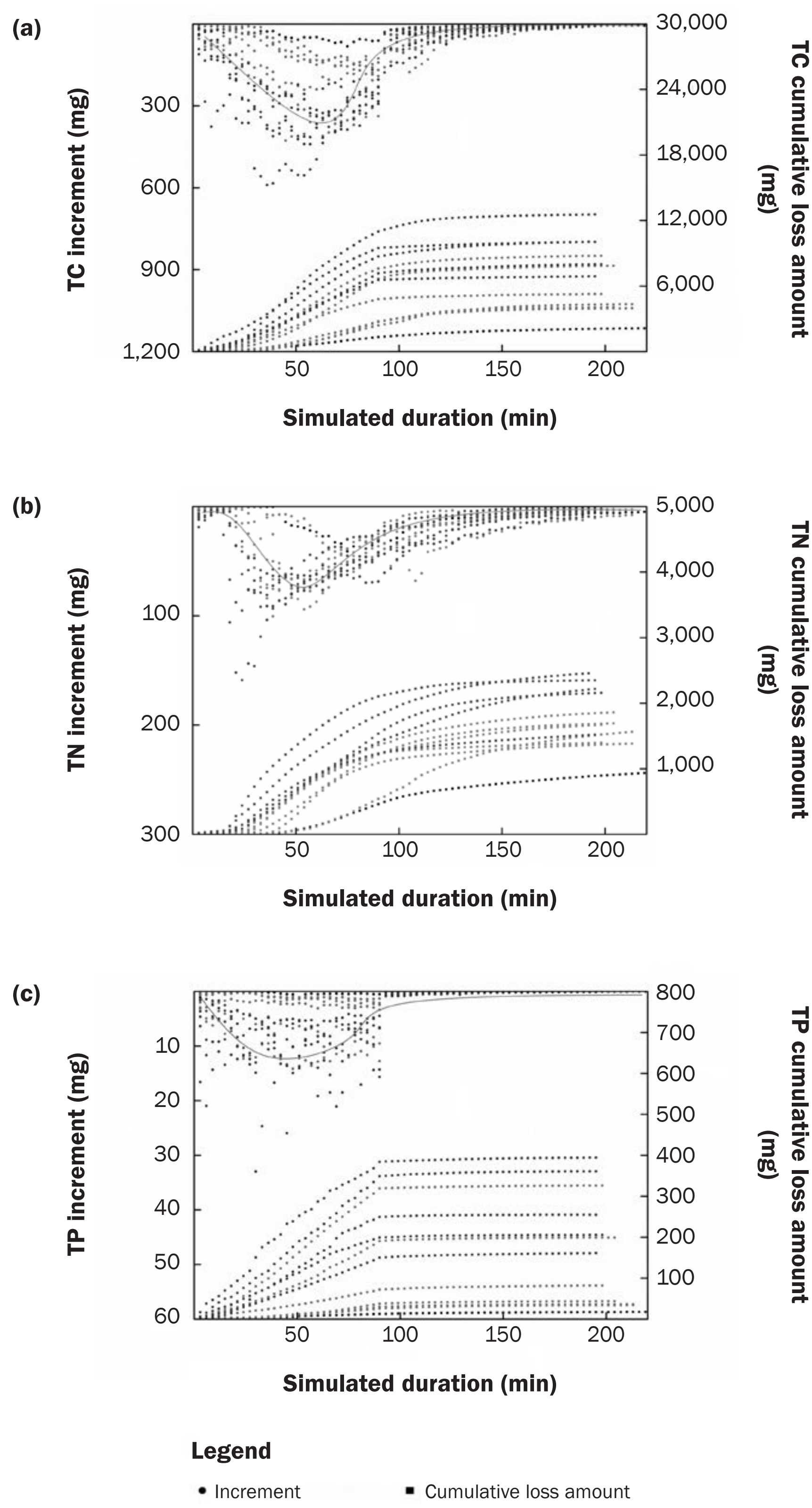

Table 2
Carbon (TC):nitrogen (TN):phosphorus (TP) ratio in soil after rainfall.

Project	TC	TP	TN
Initial ratio	6.87	1.11	1
I90-G5	6.68	1.15	1
I90-G8	6.65	1.18	1
I90-G15	6.54	1.18	1
I90-G25	6.63	1.07	1
I120-G5	6.53	1.08	1
I120-G8	6.28	1.01	1
I120-G15	6.40	0.88	1
I120-G25	6.44	0.65	1
I150-G5	6.45	0.80	1
I150-G8	6.50	0.71	1
I150-G15	6.36	0.66	1
I150-G25	5.98	0.26	1

Figure 7
(a) Ratio of total carbon (TC), total nitrogen (TN), and total phosphorus (TP) loss gross amounts with interflow and overland flow and (b) ratio of TC, TN, and TP loss gross amounts with rainfall induced runoff (RIR) and sediment.

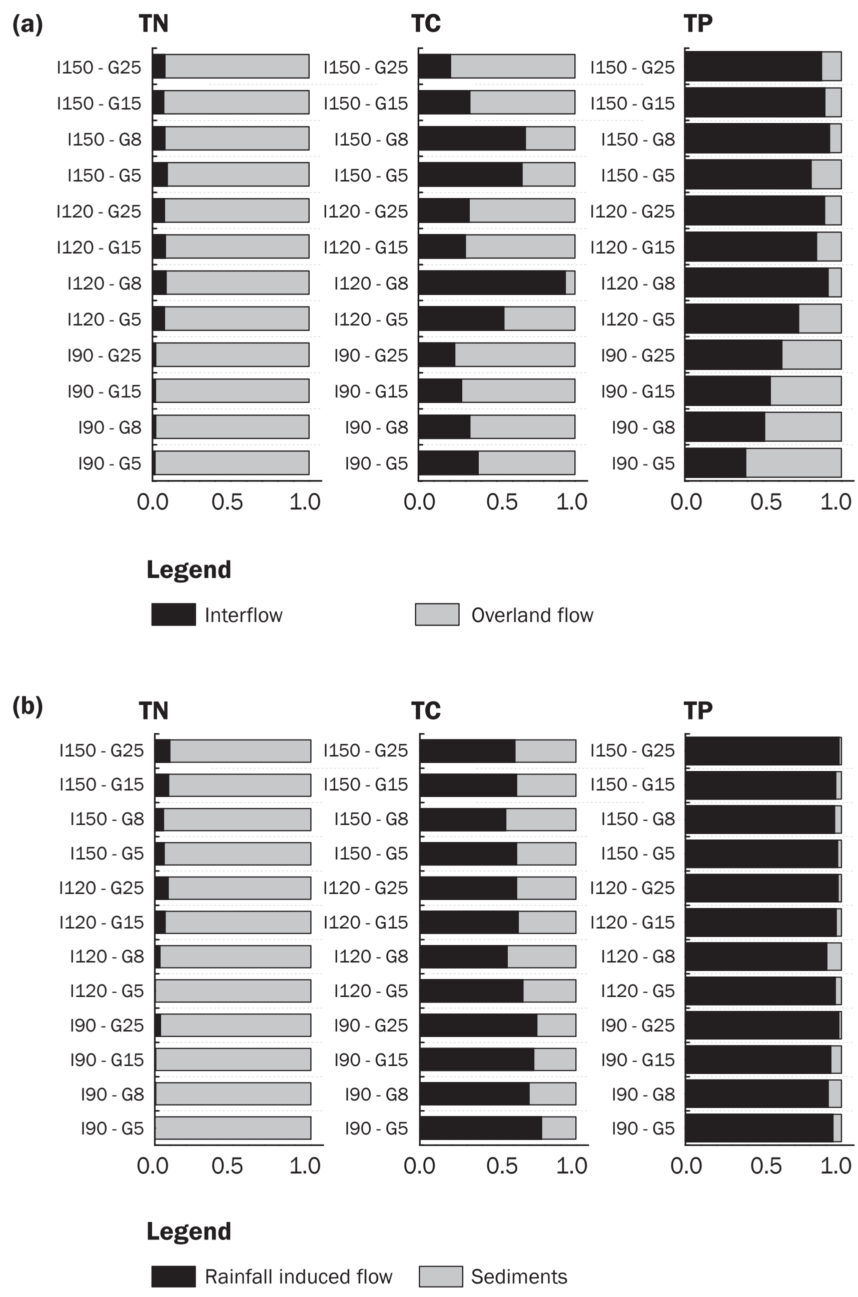

Our results indicated that rainfall would reduce C:N ratios on sloped land. The C:N ratio is a sensitive indicator of soil quality, and C:N ratio will affect the circulation of organic C and N in the soil. The lower the C:N ratio, the higher the available N content (Deng et al. 2020b). When the C:N ratio decreases, excessive soil N sources are prone to release, which would boost the content of NH_4^+-N or NO_3-N and accelerate the N loss with runoff and sediment (Aanderud et al. 2018).

Carbon to phosphorus ratios can be used as an effective index of soil P saturation. Soil C:P ratio can be used as an indicator to measure the potential of microbial mineralized soil organic matter to release P or absorb and retain P from the environment (Tipping et al. 2016). This study showed the C:P ratio decreased after smaller rainfall intensity and increased after larger rainfall intensity. Phosphorus is mostly absorbed in the soil. When the rainfall intensity increases, more sediments will be lost. The amount of P loss with the sediment is much greater than the RIR, so when the rain is strong, C:P ratio will increase rapidly. At the same time, C:P ratio has a larger variation range than C:N ratio, which is caused by the source of soil P (Wang et al. 2017). The C:P ratio obtained in this study ranges from 5.54 to 23, which is much larger than C:N ratio variation range. Soil C:P ratio is an important indicator for judging the release or absorption of P during the mineralization of organic C. It is inversely related to the potential of P release from microorganisms. When C:P ratio is lower, it will have stronger P release ability, and when C:P ratio is higher, it will cause assimilation. There is a competitive relationship between soil microorganisms and plants, which hold the absorbed P in the soil (Zhu et al. 2014).

This study showed that the change trend of the N:P ratio was similar with that of the C:P ratio. The N:P ratio can be used to find the threshold of nutrient limitation. It can also be used as an important indicator to determine whether N is saturated (Carnicer et al. 2015). The N and P that can be absorbed by plants in the soil are available N and available P. The soil N:P ratio reflects the measurement ratio of the total N and total P content in the soil, so the N:P ratio has a certain degree in the diagnosis of soil nutri-

Figure 8

Correlation analysis of rainfall intensity, slope gradient, and total carbon (TC), total nitrogen (TN), and total phosphorus (TP) predicted value with (a) TC, (b) TN, and (c) TP loss gross amounts. I is the relationship between rainfall intensity and TC, TN, and TP loss gross amounts; S is the relationship between slope gradient and TC, TN, and TP loss gross amounts; and L is the relationship between TC, TN, and TP predicted value and their measured values.

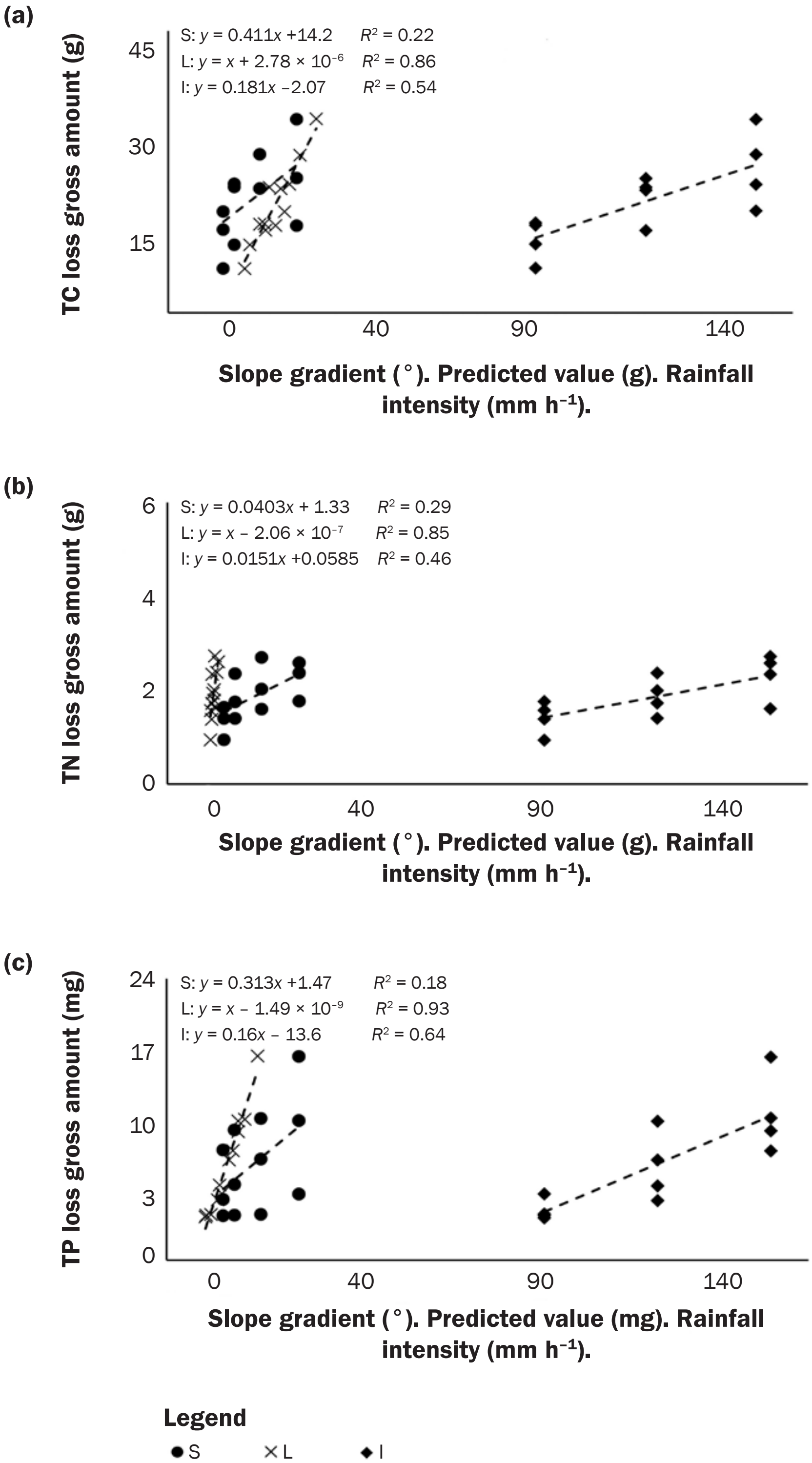

ents' limitation. However, soil N:P ratio can reflect the soil nutrient capacity and soil N and P mineralization rate to a certain extent, thereby indirectly predicting the supply level and restriction of community nutrients (Yue et al. 2017).

Nutrient Transport by Sediment and Rainfall Induced Runoff. Part of the soluble or suspended nutrient is lost with RIR, and the other part is absorbed in eroded sediments (Bertol et al. 2007). For TN and TP, the results obtained in this study were similar with those of other studies. TN was lost more with RIR, and TP was lost more with sediments. The lost N and P will enter the waterways and serve as one of the sources that cause eutrophication (Miller et al. 2011; Tuukkanen et al. 2017). Previous studies have shown that growing plants on slopes is the most cost-effective way to prevent nutrient loss due to rainfall (Cerdan et al. 2002), but the selection of optimal plants in different regions is still unclear. This will be the focus of our future research.

TC loss in this study differs from that reported in other studies. Most studies report that C will be lost with sediments rather than RIR, because soluble C only accounts for a negligible part of TC as less than 1% (Jin et al. al. 2009; Liu et al. 2018). However, this study found that in the case of fertilization, the TC lost with RIR was so large that it could not be ignored and accounted for more than 10% of the total loss. According to the ordinary C testing method in water, it is necessary to take the supernatant of the water sample for detection or measure after filtering through a 0.45 um membrane. Under this method, only the C content in the colloid and the solution content can be determined. Therefore, we tried not to filter the membrane, and we found that the TC mass concentration was large in this case. There should be three parts in this concentration. One part is the dissolved C in the RIR. One part is the suspended and particulate C, which will be lost with the RIR when the flow velocity reaches the initial velocity. Another part is C in extremely fine-grained sediments transported by RIR. Therefore, this experiment demonstrated that when the rainfall is strong enough or the flow velocity is fast, a large amount of C will be lost with RIR instead of just the soluble C. This phenomenon was also observed in our previous study; the amount of TC lost with RIR on the laterite soil layer slopes and surface soil layer slopes cannot be ignored (Fei et al. 2019).

Summary and Conclusion

Since the rainstorm erosion process may aggravate the loss of chemical fertilizer, choosing an appropriate fertilization time and application method is very important to prevent nutrient loss and contamination of waterways. TC, TN, and TP loss rates and mass concentration under simulated rainfall were studied, as TC, TN, and TP loss gross amounts in RIR and sediments were studied simultaneously. We also applied correlation analysis and simple stoichiometry for data analysis. These conclusions provide some theoretical basis for nutrient loss from slopes in decomposed granite soil areas, with the following results:

1. Large TN and TP mass concentrations in OF were measured only at the beginning of each test, then decreased rapidly with the increase of OF duration. Large TC mass concentration was observed at the beginning of each test with large OF volume and in the middle and later periods of test duration with smaller OF volume.
2. TC, TN, and TP mass concentration in IF decreased with the increase of IF duration. Larger TN and TP mass concentrations were mainly distributed with small IF volume at the initial period of IF duration, while higher TC mass concentration was distributed with larger IF volume.
3. TC, TN, and TP cumulative loss amounts increased rapidly with the increase of simulated duration and then increased slowly, as the inflection point appeared at the end time of rainfall.
4. Nutrient loss with RIR and sediments reduced C:N of the soil and increased C:P and N:P when the rainfall intensity was 120 or 150 mm h^{-1}.
5. Sediments were the main carrier of TC and TP, and RIR was the main carrier of TN. In RIR, TP was mainly lost with OF, TN was mainly lost with IF, and TC was lost less with OF when the slope was steeper.
6. TC, TN, and TP loss gross amounts all had significant linear dependence with rainfall intensity and slope gradient.

Acknowledgements

Funding for this work was supported by the National Natural Science Foundation of China (No. 41877065). In addition, Kai Fei especially hopes to express his respect to Kobe Bryant and his Mamba mentality, which keeps inspiring him to move forward.

References

Aanderud, Z.T., S. Saurey, B.A. Ball, D.H. Wall, J.E. Barrett, M.E. Muscarella, N.A. Griffin, et al. 2018. Stoichiometric shifts in soil C: N: P promote bacterial taxa dominance, maintain biodiversity, and deconstruct community assemblages. Frontiers in Microbiology 9:1401.

Ågren, G.I., and M. Weih. 2012. Plant stoichiometry at different scales: Element concentration patterns reflect environment more than genotype. New Phytologist 194(4):944-952.

Bao, S.D. 2000. Method for determination of soil physical and chemical properties. Chinese Soil and Agricultural Chemistry Analysis 22–107.

Bertol, I., F.L. Engel, A.L. Mafra, O.J. Bertol, and S.R. Ritter. 2007. Phosphorus, potassium and organic carbon concentrations in runoff water and sediments under different soil tillage systems during soybean growth. Soil & Tillage Research 94(1):142-150.

Boddy, E., P.W. Hill, J. Farrar, and D.L. Jones. 2007. Fast turnover of low molecular weight components of the dissolved organic carbon pool of temperate grassland field soils. Soil Biology & Biochemistry 39:827–835.

Bouyoucos, G.J. 1962. Hydrometer method improved for making particle size analyses of soils 1. Agronomy Journal 54(5):464-465.

Bremner, J. 1960. Determination of nitrogen in soil by the Kjeldahl method. The Journal of Agricultural Science 55(1):11-33.

Brookshire, E.N.J., H.M. Valett, and S. Gerber. 2009. Maintenance of terrestrial nutrient loss signatures during in-stream transport. Ecology 90(2):293-299.

Carnicer, J., J. Sardans, C. Stefanescu, A. Ubach, M. Bartrons, D. Asensio, and J. Peuelas. 2015. Global biodiversity, stoichiometry and ecosystem function responses to human-induced C–N–P imbalances. Journal of Plant Physiology 172:82-91.

Cerdan, O., Y.L. Bissonnais, A. Couturier, H. Bourennane, and V. Souchère. 2002. Rill erosion on cultivated hillslopes during two extreme rainfall events in Normandy, France. Soil & Tillage Research 67(1):99-108.

Chang, B., B. Wherley, J.A. Aitkenhead-Peterson, and K.J. McInnes. 2021. Effects of urban residential landscape composition on surface runoff generation. Science of the Total Environment 783:146977.

Chaplot, V.A., and Y. Le Bissonnais. 2003. Runoff features for interrill erosion at different rainfall intensities, slope lengths, and gradients in an agricultural loessial hillslope. Soil Science Society of America Journal 67(3):844-851.

Chen, H., M. Shao, and Y. Li. 2008. The characteristics of soil water cycle and water balance on steep grassland under natural and simulated rainfall conditions in the Loess Plateau of China. Journal of Hydrology 360(1-4):242-251.

Cleveland, C.C., and D. Liptzin. 2007. C: N: P stoichiometry in soil: Is there a "Redfield ratio" for the microbial biomass? Biogeochemistry 85(3):235-252.

Deng, L., T. Sun, K. Fei, L. Zhang, X. Fan, Y. Wu, and L. Ni. 2020a. Effects of erosion degree, rainfall intensity and slope gradient on runoff and sediment yield for the bare soils from the weathered granite slopes of SE China. Geomorphology 352:106997.

Deng, X., W. Ma, Z. Ren, M. Zhang, M.L. Grieneisen, X. Chen, X. Fei, et al. 2020b. Spatial and temporal trends of soil total nitrogen and C/N ratio for croplands of East China. Geoderma 361:114035.

Du, C., and Y. Gao. 2021. Grazing exclusion alters ecological stoichiometry of plant and soil in degraded alpine grassland. Agriculture, Ecosystems & Environment 308:107256.

Duan, X., Y. Deng, Y. Tao, Y. He, L. Lin, and J. Chen. 2021. The soil configuration on granite residuals affects Benggang erosion by altering the soil water regime on the slope. International Soil and Water Conservation Research 9(3):419-432.

Fei, K., L. Deng, T. Sun, L. Zhang, Y. Wu, X. Fan, and Y. Dong. 2019. Runoff processes and lateral transport of soil total carbon induced by water erosion in the hilly region of southern China under rainstorm conditions. Geomorphology 340:143-152.

Fujimoto, M., N. Ohte, and M. Tani. 2007. Effects of hillslope topography on hydrological responses in a weathered granite mountain, Japan: Comparison of the runoff response between the valley-head and the side slope. Hydrological Process 22(14):2581-2594.

Goel, M.K. 2011. Interflow. *In* Encyclopedia of Snow, Ice and Glaciers, ed. V.P. Singh, P. Singh, U.K. Haritashya, 647. Encyclopedia of Earth Sciences Series. Dordrecht: Springer. https://doi.org/10.1007/978-90-481-2642-2_298.

Gomez-Gonzalez, M.A., A. Voegelin, J. Garcia-Guinea, E. Bolea, F. Laborda, and F. Garrido. 2016. Colloidal mobilization of arsenic from mining-affected soils by surface runoff. Chemosphere 144:1123-1131.

Huang, J., Z. Li, P. Zhang, J. Liu, D. Cheng, F. Ren, Z. Wang. 2017. CO_2 emission pattern of eroded sloping croplands after simulated rainfall in subtropical China. Ecological Engineering 99:39-46.

Huang, J., P. Wu, and X. Zhao. 2013. Effects of rainfall intensity, underlying surface and slope gradient on soil infiltration under simulated rainfall experiments. Catena 104:93-102.

Jahn, R., H. Blume, V. Asio, O. Spaargaren, and P. Schad. 2006. Guidelines for Soil Description. Rome: Food and Agriculture Organization of the United Nations.

Jiang, Y.H., C.Y. Ha, and Y.D. Lu. 2010. Environmental Geology of Southeast Coast and Important Economic Zone. Beijing: Geological Publishing House (Chinese).

Jin, K., W.M. Cornelis, D. Gabriels, M. Baert, H.J. Wu, W. Schiettecatte, D.X. Cai, et al. 2009. Residue cover and rainfall intensity effects on runoff soil organic carbon losses. Catena 78(1):0-86.

Katsuyama, M., M. Tani, and S. Nishimoto. 2010. Connection between stream water mean residence time and bedrock groundwater recharge/discharge dynamics in weathered granite catchments. Hydrological Process 24(16):2287-2299.

Kleinman, P.J., M.S. Srinivasan, C.J. Dell, J.P. Schmidt, A.N. Sharpley, and R.B. Bryant. 2006. Role of rainfall intensity and hydrology in nutrient transport via surface runoff. Journal of Environmental Quality 35(4):1248-1259.

Korkanç, S.Y., and G. Dorum. 2019. The nutrient and carbon losses of soils from different land cover systems under simulated rainfall conditions. Catena 172:203-211.

Lang, M., P. Li, and X. Yan. 2013. Runoff concentration and load of nitrogen and phosphorus from a residential area in an intensive agricultural watershed. Science of the Total Environment 458:238-245.

Lee, J.H., and K.W. Bang. 2000. Characterization of urban stormwater runoff. Water Research 34(6):1773-1780.

Liu, L., Z.W. Li, X.F. Chang, X.D. Nie, and D.Y. Wang. 2018. Relationships of the hydraulic flow characteristics with the transport of soil organic carbon and sediment loss in the Loess Plateau. Soil & Tillage Research 175:291-301.

Liu, L., Z.W. Li, X.D. Nie, J.J. He, B. Huang, X.F. Chang, C. Liu, H.B. Xiao, and D.Y. Wang. 2017. Hydraulic-based empirical model for sediment and soil organic carbon loss on steep slopes for extreme rainstorms on the Chinese Loess Plateau. Journal of Hydrology 554:600-612.

Ma, T., C. Li, Z. Lu, and Q. Bao. 2015. Rainfall intensity–duration thresholds for the initiation of landslides in Zhejiang Province, China. Geomorphology 245:193–206.

Miller, J.J., D.S. Chanasyk, T.W. Curtis, and B.M. Olson. 2011. Phosphorus and nitrogen in runoff after phosphorus- or nitrogen-based manure applications. Journal of Environmental Quality 40(3):949.

Petry, J., C. Soulsby, I.A. Malcolm, and A.F. Youngson. 2002. Hydrological controls on nutrient concentrations and fluxes in agricultural catchments. Science of the Total Environment 294:95–110.

Qian, J., L.P. Zhang, W.Y. Wang, and Q. Liu. 2014. Effects of vegetation cover and slope length on nitrogen and phosphorus loss from a sloping land under simulated rainfall. Polish Journal of Environmental Studies 23(3):835-843.

Ramos, M.C., I. Lizaga, L. Gaspar, L. Quijano, and A. Navas. 2019. Effects of rainfall intensity and slope on sediment, nitrogen and phosphorous losses in soils with different use and soil hydrological properties. Agricultural Water Management 226:105789.

Rimal, B.K., and R. Lal. 2009. Soil and carbon losses from five different land management areas under simulated rainfall. Soil & Tillage Research 106(1):62-70.

Ross, D.J., K.R. Tate, N.A. Scott, and C.W. Feltham. 1999. Land-use change: Effects on soil carbon, nitrogen and phosphorus pools and fluxes in three adjacent ecosystems. Soil Biology & Biochemistry 31(6):0-813.

Ruby, M.V., Y.W. Lowney, A.L. Bunge, S.M. Roberts, J.L. Gomez-Eyles, U. Ghosh, J.C. Kissel, P. Tomlinson, and C. Menzie. 2016. Oral bioavailability, bioaccessibility, and dermal absorption of PAHs from soil: State of the science. Environmental Science & Technology 50(5):2151-2164.

Schipper, L.A., H.J. Percival, and G.P. Sparling. 2004. An approach for estimating when soils will reach maximum nitrogen storage. Soil Use and Management 20(3):281-286.

Shen, Z., L. Chen, X. Ding, Q. Hong, and R. Liu. 2013. Long-term variation (1960–2003) and causal factors of non-point-source nitrogen and phosphorus in the upper reach of the Yangtze River. Journal of Hazardous Materials 252-253:45-56.

Tipping, E., C.J. Somerville, and J. Luster. 2016. The C: N: P: S stoichiometry of soil organic matter. Biogeochemistry 130(1-2):117-131.

Tiwari, K.R., B.K. Sitaula, R.M. Bajracharya, and T. Børresen. 2010. Effects of soil and crop management practices on yields, income and nutrients losses from upland farming systems in the Middle Mountains region of Nepal. Nutrient Cycling in Agroecosystems 86(2):241-253.

Tuukkanen, T., H. Marttila, and B. Kløve. 2017. Predicting organic matter, nitrogen, and phosphorus concentrations in runoff from peat extraction sites using partial least squares regression. Water Resources Research 53(7):5860-5876.

Wang, G., B. Wu, L. Zhang, H. Jiang, and Z. Xu 2014. Role of soil erodibility in affecting available nitrogen and phosphorus losses under simulated rainfall. Journal of Hydrology 514:180-191.

Wang, L., N. Dalabay, P. Lu, and F. Wu. 2017. Effects of tillage practices and slope on runoff and erosion of soil from the Loess Plateau, China, subjected to simulated rainfall. Soil & Tillage Research 166:147-156.

Wang, M., and T.R. Moore. 2014. Carbon, nitrogen, phosphorus, and potassium stoichiometry in an ombrotrophic peatland reflects plant functional type. Ecosystems 17(4):673-684.

Wang, Q., S. Ding, D. Xia, Y. Deng, X. Ye, D. Liu, and J. Xu. 2016. Quantitative research of different soil layers detachment rate in Granite Collapse region. Journal of Soil and Water Conservation 30(3):65-70.

Wu, L., S. Qiao, M. Peng, and X. Ma. 2018. Coupling loss characteristics of runoff-sediment-adsorbed and dissolved nitrogen and phosphorus on bare loess slope. Environmental Science and Pollution Research 25(14):14018-14031.

Wu, L., H. Yen, and X. Ma. 2021. Effects of particulate fractions on critical slope and critical rainfall intensity for runoff phosphorus from bare loessial soil. Catena 196:104935.

Xu, T., X. Sun, H. Hong, X. Wang, M. Cui, G. Lei, L. Gao, et al. 2019. Stable isotope ratios of typhoon rains in Fuzhou, Southeast China, during 2013–2017. Journal of Hydrology 570:445-453.

Xu, X., F. Zheng, G. Wilson, C. He, J. Lu, and F. Bian. 2018. Comparison of runoff and soil loss in different tillage systems in the Mollisol region of Northeast China. Soil & Tillage Research 177:1-11.

Yue, K., D.A. Fornara, W. Yang, Y. Peng, and C. Peng. 2017. Effects of three global change drivers on terrestrial C:N:P stoichiometry: A global synthesis. Global Change Biology 23(6):2450-2463.

Zhang, L., R. Zhang, and Y. Wu. 2017. A new variable slope three-dimensional monitoring runoff flume. Chinese Patent CN206096119U, 2017-04-12.

Zheng, S., S.D.N. Lourenco, P.J. Cleall, T.F.M. Chui, A.K.Y. Ng, and S.W. Millis. 2017. Hydrologic behavior of model slopes with synthetic water repellent soils. Journal of Hydrology 554:582-599.

Zhu, Q., W. Riley, J. Chambers, and J. Tang. 2014. Modeling plant, microorganisms, and mineral surface competition for soil nitrogen and phosphorus: Competition representations and ecological significance. AGU Fall Meeting Abstracts, San Francisco, California.